nature chemistry

SUPPLEMENTARY INFORMATION

DOI: 10.1038/NCHEM.1873

Discovery of a Ni-Ga catalyst for carbon dioxide reduction to methanol

Felix Studt,[1] Irek Sharafutdinov,[2] Frank Abild-Pedersen,[1] Christian F. Elkjær,[2] Jens S. Hummelshøj,[1] Søren Dahl,[2] Ib Chorkendorff,[2] and Jens K. Nørskov[1,3*]

1 SUNCAT Center for Interface Science and Catalysis, SLAC National Accelerator Laboratory, 2575 Sand Hill Road, Menlo Park, CA 94025 (USA)

2 Center for Individual Nanoparticle Functionality (CINF), Department of Physics, Building 307 Technical University of Denmark, DK-2800 Lyngby, Denmark

3 SUNCAT Center for Interface Science and Catalysis, Department of Chemical Engineering, Stanford University, Stanford, CA 94305 (USA)

Energies of adsorbates and transition states:

Table S1. RPBE adsorption energies of intermediates without and with zero point energy correction. Corrections are based on vibrational calculations on the Cu(211) surface alone. All energies are shown in eV and given relative to CH_4, H_2O and H_2 in the gas phase.

Uncorr.	Surface*				
Adsorbate	Ag(211)	Cu(211)	Pd(211)	Pt(211)	Rh(211)
H*	0.31	-0.12	-0.34	-0.54	-0.44
O*	1.92	1.03	1.54	1.30	0.20
OH*	0.57	0.12	0.69	0.30	-0.26
HCOO*	2.02	1.57	1.99	1.85	1.17
HCOOH*	2.60**				
H_2COOH*	2.51	2.01	2.37	2.62	2.06
H_2CO*	2.40	2.35	1.92	1.77	1.43
H_3CO*	1.89	1.34	1.72	1.53	1.04

ZPE corr.	Surface				
Adsorbate	Ag(211)	Cu(211)	Pd(211)	Pt(211)	Rh(211)
H*	0.34	-0.09	-0.31	-0.51	-0.41
O*	1.70	0.81	1.32	1.08	-0.02
OH*	0.50	0.05	0.62	0.23	-0.33
HCOO*	1.29	0.84	1.26	1.12	0.44
HCOOH*	2.01**				
H_2COOH*	2.12	1.62	1.98	2.23	1.67
H_2CO*	1.75	1.70	1.27	1.12	0.78
H_3CO*	1.64	1.09	1.47	1.28	0.79

**Similar data for some intermediates can found in the CatApp.[1] That data was obtained on a slightly different surface and slightly different computational setup thus deviating slightly from the energies presented here. **The HCOOH adsorption energy is zero for all surfaces when calculated with the RPBE functional.*

Table S2. RPBE transition state energies without and with zero point energy correction. Corrections are based on vibrational calculations on the Cu(211) surface alone. All energies are shown in eV and given relative to CH_4, H_2O and H_2 in the gas phase.

Uncorr.	Surface*				
Transition state	Ag(211)	Cu(211)	Pd(211)	Pt(211)	Rh(211)
H-H	1.40	0.74	0.00		0.00
H-COO	3.47	2.89	2.99	2.87	2.63
HCOO-H	2.89	2.76	2.76	2.63	1.46
H-HCOOH	3.56	2.87	2.59	2.78	2.93
H_2CO-OH	2.97	2.08	2.60	2.07	1.18
H-H_2CO	3.07	2.56	2.40	2.15	1.72
H_3CO-H	2.98	2.03	2.41	2.12	1.85
HO-H	1.75	0.82	1.20	0.95	0.63

ZPE corr.	Surface*				
Transition state	Ag(211)	Cu(211)	Pd(211)	Pt(211)	Rh(211)
H-H	1.40	0.74	0.00		0.00
H-COO	2.51	1.93	2.03	1.91	1.67
HCOO-H	2.10	1.97	1.97	1.84	0.67
H-HCOOH	2.99	2.30	2.02	2.21	2.36
H_2CO-OH	2.49	1.60	2.12	1.59	0.70
H-H_2CO	2.62	2.11	1.95	1.70	1.27
H_3CO-H	2.69	1.74	2.12	1.83	1.56
HO-H	1.65	0.72	1.10	0.85	0.53

**Similar data for some intermediates can found in the CatApp.[1] That data was obtained on a slightly different surface and slightly different computational setup thus deviating slightly from the energies presented here.*

Scaling relations

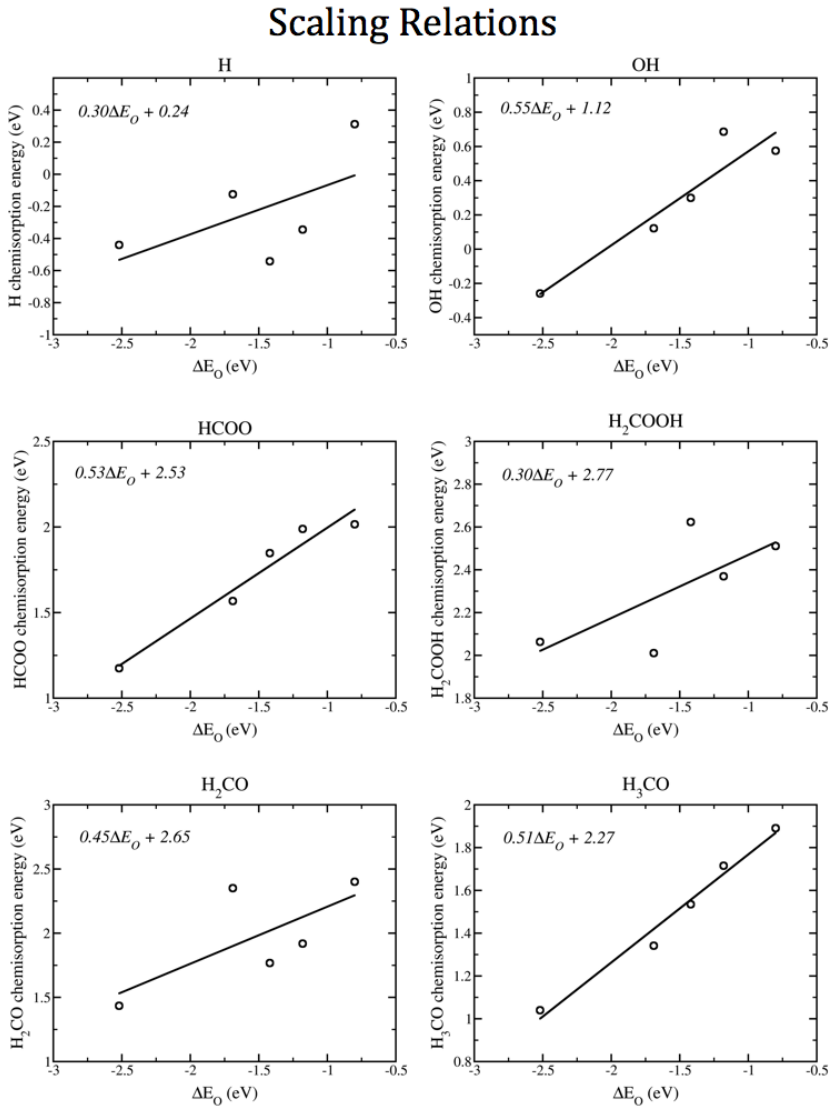

Figure S1. Scaling relations for all adsorbates as a function of ΔE_O. All energies are relative to CH_4, H_2O and H_2 in the gas-phase.

Transition state scaling relations

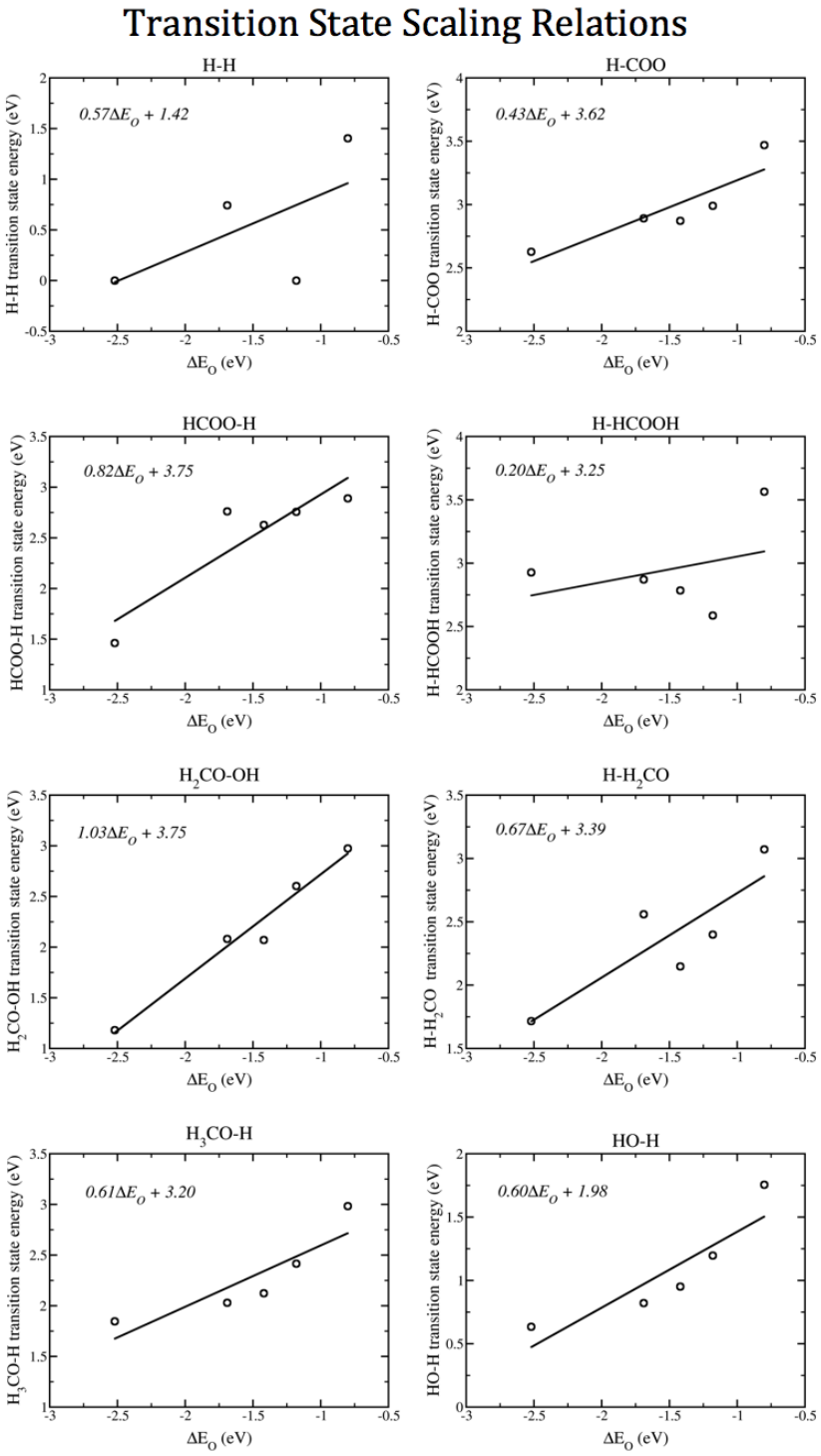

Figure S2. Scaling relations for all transition-states as a function of ΔE_O. All energies are relative to CH_4, H_2O and H_2 in the gas-phase.

Calculations of active surface area:

Estimation of the active surface area was done based on the results from XRD and TEM investigations. The corresponding data is summarized in table S3 below:

Table S3

catalyst	particle size, TEM nm	particle size, XRD, nm	metal surface area, TEM, m^2	metal surface area, XRD, m^2
$NiGa/SiO_2$	6.2	7.1	8.9	7.6
Ni_5Ga_3/SiO_2	5.1	5.9	10.6	9.2
Ni_3Ga/SiO_2	N/A	4.8	N/A	10.9
$Cu/ZnO/Al_2O_3$	N/A	5.7	N/A	9.5

For each diffractogram presented in figure 2, the FWHM (full width at half maximum) values of the most intense diffraction peak was used to calculate the average crystallite size, according to the Scherrer equation. Average TEM particle size was derived by statistical treatment of 219 and 168 particles in case of Ni_5Ga_3 and NiGa, respectively. Note that the values of active surface area for the two most active catalysts, namely Ni_5Ga_3/SiO_2 and $Cu/ZnO/Al_2O_3$ are similar, implying that their turnover frequency values are also comparable.

Reverse Water-Gas-Shift volcano

In an attempt to understand the differences in methanol/CO selectivity we constructed a rWGS activity volcano, which is shown in Figure S3. The volcano is constructed assuming ΔE_O to be fixed at the value found at the top of the methanol volcano, leaving ΔE_{CO} as the only parameter. The surface structures of NiGa and Ni_5Ga_3 exhibit both a Ni rich and a Ga rich step site. Importantly, the CO adsorption energy on the Ni rich steps on both, NiGa and Ni_5Ga_3 is -1.67 and -1.60 eV, respectively, close to that found for pure Ni.[3]. We rationalize that these sites will hence be blocked by CO under reaction conditions. Methane formation via splitting of CO is also possible although at rather low rates. This will form carbonaceous species which in turn will poison the surface. Assuming that CO_2 hydrogenation proceeds at a different site (namely the Ga site where ΔE_O is close to that of Cu, see Figure 1) one could imagine that the sites responsible for rWGS and methanation are either blocked by CO or deactivated by carbon deposition whereas this effect will be much smaller for the methanol formation sites resulting in a high methanol selectivity.

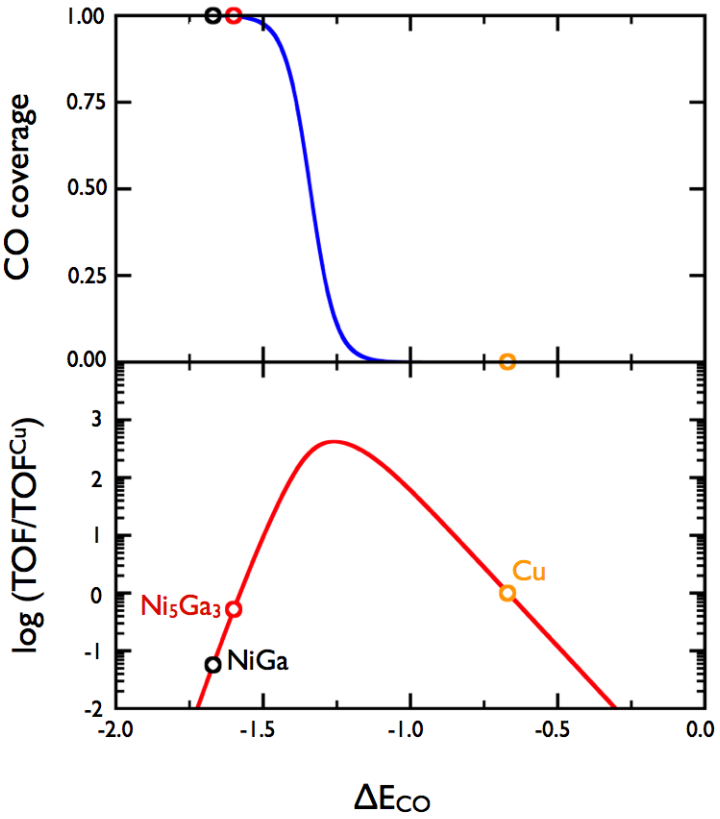

Figure S3. CO coverage (top) and rWGS activity (bottom) as a function of ΔE_{CO}. CO adsorption energies on stepped Cu, the Ni step in NiGa and the Ni step in Ni_5Ga_3 are depicted. Reaction conditions are: 500 K, 0.245 bar CO_2, 0.745 bar H_2, 0.005 bar CO and 0.005 bar H_2O.

Methane detection upon regeneration of the catalyst in H_2

Upon heating in hydrogen 0.0000235 mol of CH_4 were released which we calculated (using an average surface diameter of 5.1 nm) to be correlated to poisoning of ~ 10 % of the surface area of the catalyst. This is assuming uniform spherical Ni_5Ga^3 nanoparticles, with surface composition corresponding to that of the bulk. This is consistent with poisoning of surface step sites and we therefore suggest that catalysts deactivation occurs via carbon deposition on steps

Adsorption of CO and O on Ni_5Ga_3, Ni_3Ga, and NiGa

Ni_5Ga_3

We calculated adsorption of CO and O on Ni_5Ga_3 in the experimentally found crystal structure (space group).[4] Further information about the structure of Ni_5Ga_3 can be found at: https://materialsproject.org/materials/mp-11398/). In order to simulate adsorption on a stepped surface we cut the crystal in the (111) direction. CO and oxygen adsorption were calculated trying 10 and 6 different adsorption sites on the (111) steps, respectively. CO was found to bind most strongly at the pure Ni step (-1.6 eV). Oxygen binds most strongly at the mixed Ni-Ga step (-2.3 eV) (see Figure S4).

The DFT calculations on the Ni_5Ga_3 systems were performed using Dacapo with the RPBE functional. The Brillouin zone was sampled on a (4x4x1) grid and the kinetic energy and density cutoffs were 340 Ry and 500 Ry respectively. The slab model included 6 formula units of Ni_5Ga_3 which corresponded to a slab thickness of ~8 Å or ~6 atomic layers, with the bottom ~2.5 atomic layers kept at their symmetric positions. The adsorbent coverage on the step was 1/2.

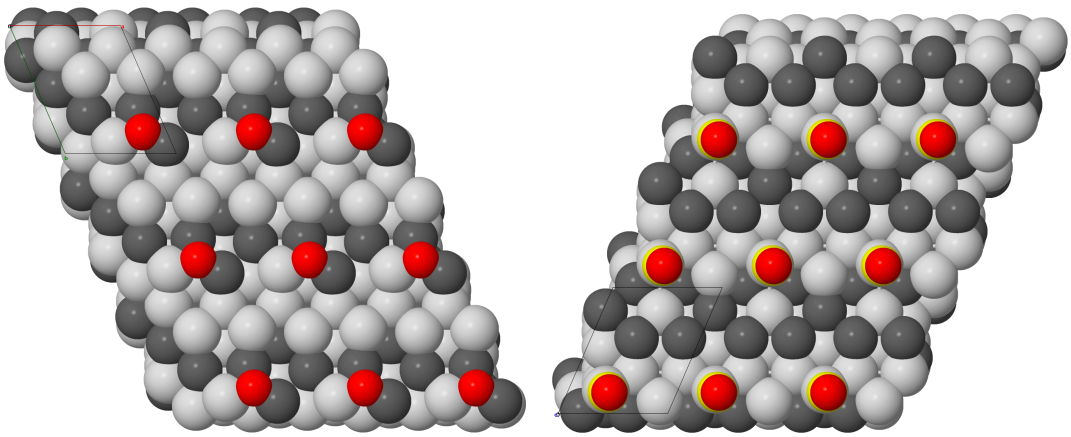

Figure S4. Adsorption of O and CO at the stepped facet of Ni_5Ga_3 (colors: Ni: dark-grey; Ga: light-grey; O: red; C: yellow). Four types of steps can form on this facet and all are represented on the figures: two types of pure Ni steps, one pure Ga and one mixed Ni-Ga. (left) O binds most strongly by -2.3eV on the mixed step (right) CO binds most strongly on the pure Ni step shown by -1.6eV.

NiGa

In order to simulate adsorption on a stepped surface of NiGa (which has a bcc structure) we cut the crystal in the (121) direction resulting in the formation of a Ni-Ni and a Ga-Ga step (see Figure S5). CO and oxygen adsorption were calculated trying 4 different adsorption sites on both steps. The calculational setup was the same as for Ni_5Ga_3 but with a density cutoff of 680 Ry and a vacuum distance of approximately 12 Å.

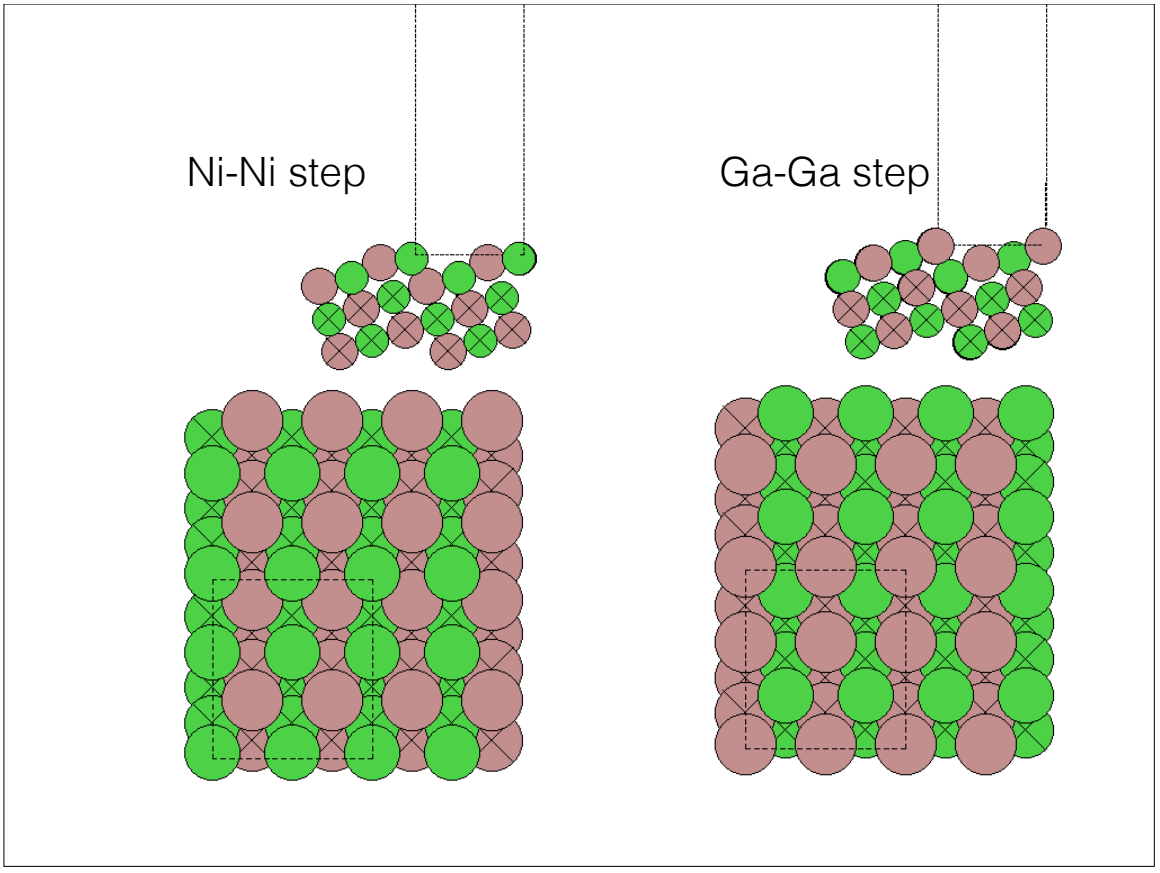

Figure S5. The Ni-Ni and Ga-Ga steps of NiGa (colors: Ni: green; Ga: brown). Two types of steps can form on this facet as represented in the figures: a pure Ni step, and a pure Ga step. The steps are shown from a side view (top) and an ontop view (bottom). The dashed line indicates the unit cell used for the calculations.

Ni_3Ga

In order to simulate adsorption on a stepped surface (which has an fcc structure) we cut the crystal in the (211) direction resulting in the formation of a Ni-Ni and a Ni-Ga step (see Figure S6). Oxygen adsorption was calculated trying 7 and 4 different adsorption sites on the (211) steps, respectively. The calculational setup was the same as for Ni_5Ga_3 but with a density cutoff of 680 Ry and a vacuum distance of 10 Å.

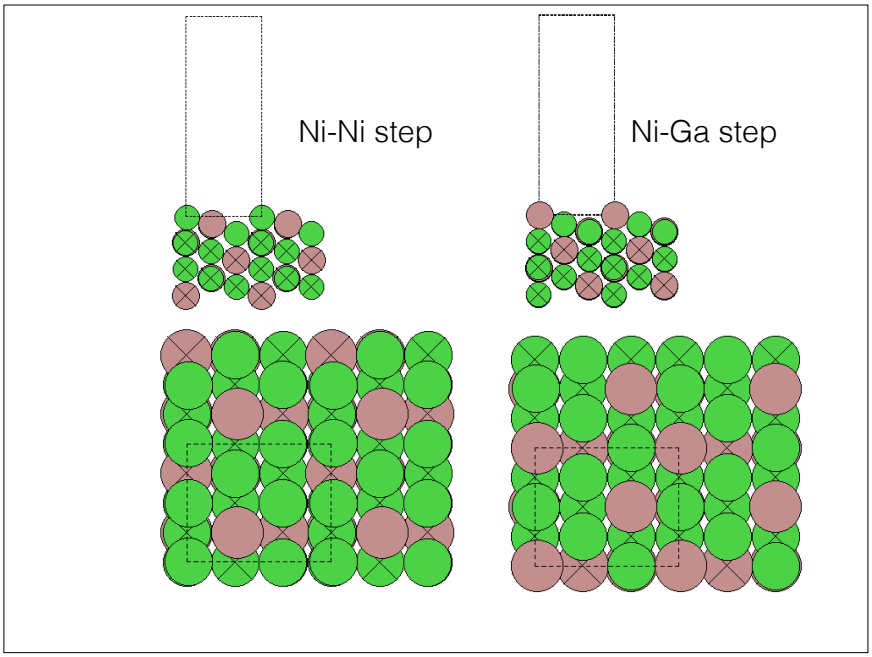

Figure S6. The Ni-Ni and Ni-Ga steps of Ni_3Ga (colors: Ni: green; Ga: brown). Two types of steps can form on this facet as represented in the figures: a pure Ni step, and a mixed Ni-Ga step. The steps are shown from a side view (top) and an ontop view (bottom). The dashed line indicates the unit cell used for the calculations.

Reference XRD data

Figure S7 displays the reference XRD data for Ni_3Ga,[6] Ni_5Ga_3,[7] and NiGa.[8]

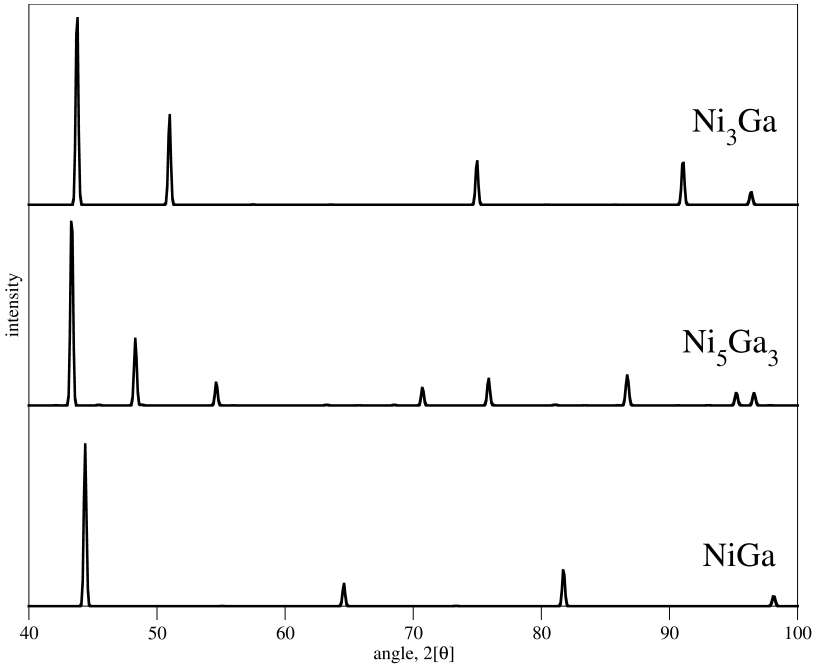

Figure S7. Reference XRD data for Ni3Ga, Ni5Ga3 and NiGa. Data from refs 6-8.

Error bar estimation for Figure 3

For all compounds detected, the representative peak area values recorded by the Gas Chromatograph (GC) at each temperature are measured 5 times by means of manual integration. Based the results of these measurements, the corresponding standard deviation values (error bars) are calculated. Then, when necessary, the standard deviation values are multiplied or divided to get the error bars of the selectivities or CO/CH_3OH ratios, using the following equations:

$$dz = (x/y)*(dx/x + dy/y) \quad \text{or} \quad dz = dx*xy$$

where:

- **dz** is the resulting error bar
- **dx** and **dy** are the individual error bars
- **x** and **y** are the values recorded by the Gas Chromatograph or calculated selectivities

Therefore, the error bars are reflecting the *intrinsic accuracy of the quantification by the GC*, but *not* the scatter of *N* data points collected and averaged at a certain temperature.
The error bars associated with CH_3OH signal and the calculated selectivities (figures 3a and 3b, respectively) appear to be 2-3 orders of magnitude smaller than the corresponding values and are therefore not shown in figures 3a and 3b. The error bars of the CO/CH_3OH ratio (figure 3c) are somewhat larger. Since the data is shown on a logarithmic plot, however, the error bars are smaller than the corresponding data points and are therefore not shown in the figure but can be found in table S4.

Ni_5Ga_3/SiO_2	Temperature in C						
	168	183	198	213	223	233	249
CO/MeOH ratio	0.845	1.10	1.23	1.94	2.61	4.97	15.0
Error bar	0.236	0.140	0.106	0.100	0.119	0.163	0.375

$Cu/ZnO/Al_2O_3$	Temperature in C				
	189	204	219	233	248
CO/MeOH ratio	1.36	2.81	7.71	34.8	225
Error bar	0.117	0.099	0.123	0.278	0.979

References

[1] Hummelshøj, J. S., Abild-Pedersen, F., Studt, F., Bligaard, T., Nørskov, J. K. CatApp: A Web Application for Surface Chemistry and Heterogeneous Catalysis. *Angew. Chem. Int. Ed.* **51**, 272-274 (2012).

[2] Baltes, C., Vukojević, S. & Schüth, F. Correlations between synthesis, precursor, and catalyst structure and activity of a large set of CuO/ZnO/Al2O3 catalysts for methanol synthesis. *J. Catal.* **258**, 334-344 (2008).

[3] Andersson, M. P., Abild-Pedersen, F., Remediakis, I. N., Bligaard, T., Jones, G., Engbæk, J., Lytken, O., Horch, S., Nielsen, J. H., Sehested, J., Rostrup-Nielsen, J. R., Nørskov, J. K. & Chorkendorff, I. Structure sensitivity of the methanation reaction: H2-induced CO dissociation on nickel surfaces. *J. Catal.* **255**, 6-19 (2008).

[4] Jain, A., Hautier, G., Moore, C., Ong, S. P., Fischer, C., Mueller, T., Persson, K., Ceder G. A high-throughput infrastructure for density functional theory calculations. *Comput. Mater. Sci.* **50**, 2295–2310 (2011).

[5] Ong, S. P., Jain, A., Hautier, G., Kocher, M., Cholia, S., Gunter, D., Bailey, D., Skinner, D., Persson, K., Ceder, G. *The Materials Project.* http://materialsproject.org/

[6] Mishima, Y., Ochiai, S. & Suzuki, T. Lattice parameters of Ni(γ), Ni3Al(γ') and Ni3Ga(γ') solid solutions with additions of transition and B-subgroup elements. *Acta Metall.* **33**, 1161-1169 (1985).

[7] Bhan, S. & Schubert, K. Über die Struktur von Phasen mit Kupfer Unterstruktur in einigen T-B Legierungen (T=Ni, Pd, Pt; B=Ga, In, Tl, Pb, Sb, Bi). *J. Less-Common Metals* **17**, 73-90 (1969).

[8] Guérin, R. & Guivarc'h, A. Metallurgical study of Ni/GaAs contacts. I. Experimental determination of the solid portion of the NiGaAs ternaryphase diagram. *J. Appl. Phys.* **66**, 2122-2128 (1989).